RSC Advances

ROYAL SOCIETY OF CHEMISTRY

www.rsc.org/advances

Graphical Abstract

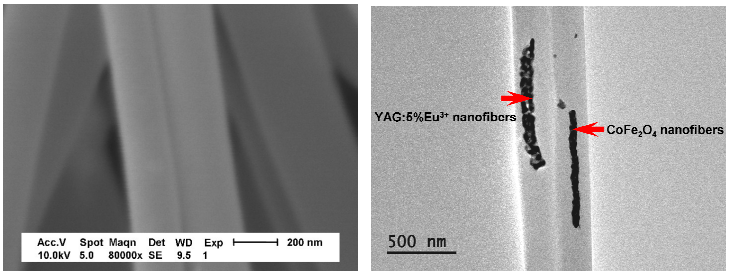

A new structure of [$CoFe_2O_4$/PVP]//[YAG:5%Eu^{3+}/PVP] magnetic-luminescent bifunctional Janus nanofibers has been successfully fabricated via electrospinning technology using a homemade parallel spinneret. [$CoFe_2O_4$/PVP]//[YAG:5%Eu^{3+}/PVP] magnetic-luminescent bifunctional Janus nanofibers possess superior magnetic and luminescent properties due to their special nanostructure, and the luminescent characteristics and saturation magnetizations of the Janus nanofibers can be tuned by adding various amounts of YAG:5%Eu^{3+} luminescent nanofibers and $CoFe_2O_4$ magnetic nanofibers. Compared with $CoFe_2O_4$/YAG:5%Eu^{3+}/PVP composite nanofibers, the magnetic-luminescent bifunctional Janus nanofibers provide higher performances due to isolating YAG:5%Eu^{3+} luminescent nanofibers from $CoFe_2O_4$ magnetic nanofibers. More importantly, the design conception and construction technology are of universal significance to fabricate other bifunctional Janus nanofibers.

Cite this: DOI: 10.1039/c0xx00000x

www.rsc.org/xxxxxx

ARTICLE TYPE

Tuned Magnetism-Luminescence Bifunctionality Simultaneously Assembled into Flexible Janus Nanofiber

Fei Bi, Xiangting Dong*, Jinxian Wang, Guixia Liu

Received (in XXX, XXX) Xth XXXXXXXXX 20XX, Accepted Xth XXXXXXXXX 20XX
DOI: 10.1039/b000000x

A new structure of [$CoFe_2O_4$/PVP]//[YAG:5%Eu^{3+}/PVP] magnetic-luminescent bifunctional Janus nanofibers has been successfully fabricated via electrospinning technology using a homemade parallel spinneret. Electrospinning-derived YAG:5%Eu^{3+} luminescent nanofibers and $CoFe_2O_4$ magnetic nanofibers are respectively incorporated into polyvinyl pyrrolidone (PVP) matrix and electrospun into Janus nanofibers with $CoFe_2O_4$ magnetic nanofibers/PVP as one strand nanofiber and YAG:5%Eu^{3+} luminescent nanofibers/PVP as another strand nanofiber. [$CoFe_2O_4$/PVP]//[YAG:5%Eu^{3+}/PVP] magnetic-luminescent bifunctional Janus nanofibers possess superior magnetic and luminescent properties due to their special nanostructure, and the luminescent characteristics and saturation magnetizations of the Janus nanofibers can be tuned by adding various amounts of YAG:5%Eu^{3+} luminescent nanofibers and $CoFe_2O_4$ magnetic nanofibers. Compared with $CoFe_2O_4$/YAG:5%Eu^{3+}/PVP composite nanofibers, the magnetic-luminescent bifunctional Janus nanofibers provide higher performances due to isolating YAG:5%Eu^{3+} luminescent nanofibers from $CoFe_2O_4$ magnetic nanofibers. More importantly, the design conception and construction technology are of universal significance to fabricate other bifunctional Janus nanofibers.

1 Introduction

Nowadays, the development of the magnetic-luminescent bifunctional nanomaterials has attracted particular interest because of their wide applications in biological systems, such as diagnostic analysis, and controlled drug release [1-5]. Most of the magnetic-luminescent nanomaterials are core-shell structures. In general, organic dyes and quantum dot (QDs) have been used as the luminescence shell of the core-shell structured magnetic-luminescent nanomaterials [6-9]. However, the photobleaching and quenching properties of organic dyes and the toxicity of QDs have seriously limited their applications. Compared with organic dyes and QDs, lanthanide-doped nanomaterials have begun to gain attention due to their excellent luminescence properties. Among these luminescent materials, Eu^{3+}-activated $Y_3Al_5O_{12}$ (YAG) is an important phosphor with a variety of applications in many luminescent and optical devices due to their excellent performance [10-13]. As a kind of magnetic materials, cobalt ferrite ($CoFe_2O_4$) has received much attention because of its moderate saturation magnetization, high coercivity and excellent physical and chemical stability, as well as its applications potentials in electronic devices, drug delivery technology, magnetic resonance imaging, and information storage [14-16].

Presently, researchers are mainly focused on the preparation, properties and applications of magnetic-luminescent bifunctional nanoparticles. In order to obtain new morphologies of magnetic-luminescent nanomaterials, the fabrication of one-dimensional (1D) magnetic-luminescent nanomaterials is an urgent subject of study.

Electrospinning is a simple and versatile technique to process polymers and related materials into one-dimensional structural fibers with controllable compositions, diameters, and porosities for a variety of applications. This method not only has attracted extensive academic investigations, but is also applied in many areas [17, 18]. By now, various magnetic-luminescent bifunctional 1D nanomaterials were prepared via electrospinning in literatures [19-21]. From these studies, it has been proved that the existence of dark-colored magnetic nanomaterials will greatly decrease the luminescence of rare earth compounds if magnetic nanomaterials are directly blended with the rare earth luminescent compounds [22-26]. Therefore, if the strong luminescence of the magnetic-luminescent bifunctional nanomaterials is to be achieved, rare earth compounds must be effectively isolated from magnetic nanomaterials in order to avoid direct contacting. In the procedure of seeking a way to ultimately reduce the impact of magnetic nanomaterials on the luminescent property of the magnetic-luminescent bifunctional nanofibers, we were inspired by the reports about the Janus particles [27-29]. Janus particles have two distinguished surfaces/chemistries on the two sides. Pierre-Gilles de Gennes, Nobel Prize in Physics winner, made the Janus particles known to the scientific community. These Janus-type morphologies allow the control of composition and of surface anisotropy, providing additional degrees of freedom in the design of composite materials. Adopting the unique feature of the asymmetry dual-sided Janus structure, Janus nanofibers can successfully help to realize the effective separation of magnetic nanomaterials from rare earth luminescent compounds, and it is expected that the Janus nanofibers simultaneously exhibits excellent magnetic and luminescent properties.

In this paper, we designed and fabricated magnetic-luminescent bifunctional [$CoFe_2O_4$/PVP]//[YAG:5%Eu^{3+}/PVP] Janus nanofibers via electrospinning using a homemade spinneret. This Janus nanostructure can successfully realize the effective separation of $CoFe_2O_4$ nanofibers from the YAG:5%Eu^{3+} nanofibers. The structure, morphology, luminescence characteristics and magnetic properties of the [$CoFe_2O_4$/PVP]//[YAG:5%Eu^{3+}/PVP] Janus nanofibers were investigated in detail, and some meaningful results were obtained.

2 Experimental Section

2.1 Chemicals

Polyvinyl pyrrolidone (PVP, M_w=1300 000) and N, N-dimethylformamide (DMF) were purchased from Tianjin Tiantai Fine Chemical Reagents Co., Ltd. HNO_3 was bought from Beijing Chemical Company. Y_2O_3 (99.99%), Eu_2O_3 (99.99%), $Al(NO_3)_3·9H_2O$, $Fe(NO_3)_3·9H_2O$ and $Co(NO_3)_2·6H_2O$ were bought from Sinopharm Chemical Reagent Co., Ltd. All chemicals were of analytical grade and directly used as received without further purification. $Y(NO_3)_3·6H_2O$ and $Eu(NO_3)_3·6H_2O$ were prepared by dissolving Y_2O_3 and Eu_2O_3 in dilute nitric acid, followed by crystallizing from the solution through evaporating the excess water and HNO_3 by heating.

2.2 Preparation of $CoFe_2O_4$ nanofibers and YAG:5%Eu^{3+} nanofibers

A traditional single-spinneret electrospinning instrument was used to prepare $CoFe_2O_4$ nanofibers (named S_1) and YAG:5%Eu^{3+} nanofibers (named S_2). In a typical procedure of preparing spinning solution for fabricating $CoFe_2O_4$ nanofibers, 1 mmol of $Fe(NO_3)_3·9H_2O$, 0.5 mmol of $Co(NO_3)_2·6H_2O$ and 2.2 g of PVP were dissolved into 15.8 g of DMF under continuous stirring. The spinning solution for preparing YAG:5%Eu^{3+} nanofibers was acquired as follows: 0.95 mmol of $Y(NO_3)_3·6H_2O$, 0.05 mmol of $Eu(NO_3)_3·6H_2O$, 1.38 g of $Al(NO_3)_3·9H_2O$ and 2.4 g of PVP were added into 15.6 g of DMF to form uniform solution under vigorous stirring. The spinning solutions were stirred for 4 h to form homogeneous mixture solutions for next-step electrospinning. Then, the spinning solutions were respectively injected into a traditional single-spinneret electrospinning setup, [$Fe(NO_3)_3$+$Co(NO_3)_2$]/PVP composite nanofibers and [$Y(NO_3)_3$+$Al(NO_3)_3$+$Eu(NO_3)_3$]/PVP composite nanofibers have been respectively prepared by electrospinning. The electrospinning parameters were as follows: the distance between the spinneret (a plastic needle) and collector was fixed at 18-20 cm and high voltage power supply was maintained at 12-15 kV. The room temperature was 20-24 °C and the relative humidity was 60%-70%. YAG:5%Eu^{3+} nanofibers and $CoFe_2O_4$ nanofibers can be obtained when the relevant composite nanofibers were annealed in air at 900 °C for 8 h and 700 °C for 4 h with the heating rate of 1 °C·min^{-1}, respectively.

2.3 Fabrication of [$CoFe_2O_4$/PVP]//[YAG:5%Eu^{3+}/PVP] Janus nanofibers and $CoFe_2O_4$/YAG:5%Eu^{3+}/PVP composite nanofibers

Two different kinds of spinning solutions were prepared to fabricate Janus nanofibers. The spinning solution for preparing the strand $CoFe_2O_4$/PVP fiber of the Janus nanofibers was acquired as follows: $CoFe_2O_4$ magnetic nanofibers (S_1) were ultrasonically dispersed in DMF for 20 min at room temperature, then a certain amount of PVP was added into the above mixture with stirring for 12 h, the final mixture was denoted as spinning solution A. In the preparation of spinning solution for fabricating the strand YAG:5%Eu^{3+}/PVP fiber of the Janus nanofibers, YAG:5%Eu^{3+} luminescent nanofibers (S_2) was added into DMF, followed by dispersing ultrasonically for 20 min, then a certain amount of PVP was dissolved into the above solution under stirring for 12 h. A mixed solution of YAG:5%Eu^{3+} nanofibers, PVP and DMF was prepared as the spinning solution B. The dosages of these materials were shown in **Table 1**.

[$CoFe_2O_4$/PVP]//[YAG:5%Eu^{3+}/PVP] Janus nanofibers were prepared using an electrospinning setup with a homemade parallel spinneret, as indicated in Fig. 1. The two kinds of spinning solutions were respectively loaded into each syringe, and the spinneret was settled vertically. A piece of flat iron net used as collector was put about 18 cm away from the tip of the plastic nozzle to collect the Janus nanofibers. A positive direct current (DC) voltage of 15 kV was applied between the spinneret and the collector. The electrospinning process was carried out at ambient temperature of 22-24 °C and relative air humidity of 60%-70%.

Meanwhile, $CoFe_2O_4$/YAG:5%Eu^{3+}/PVP composite nanofibers (named S_{b1} as shown in **Table 1**), as a contrast sample, were also prepared to study the superiority of the structure of Janus nanofibers. $CoFe_2O_4$/YAG:5%Eu^{3+}/PVP composite nanofibers were fabricated by mixing the spinning solution A1 ($CoFe_2O_4$/PVP=1:1) and the spinning solution B1 (YAG:5%Eu^{3+}/PVP=1:1) together via using a traditional single-spinneret electrospinning setup, and the spinning parameters were the same as those in the fabrication of the Janus nanofibers.

Table 1 Compositions of the spinning solution A and B

Samples	Spinning solutions	PVP/g	DMF/g	$CoFe_2O_4$ nanofibers (S_1)/g	YAG:5%Eu^{3+} nanofibers (S_2)/g
S_{a1}	A1 ($CoFe_2O_4$/PVP=1:1)	0.300	2.007	0.300	
	B1 (YAG:5%Eu^{3+}/PVP=1:1)	0.300	2.200		0.300
S_{a2}	A2 ($CoFe_2O_4$/PVP=1:3)	0.900	6.023	0.300	
	B1 (YAG:5%Eu^{3+}/PVP=1:1)	0.300	2.200		0.300
S_{a3}	A3 ($CoFe_2O_4$/PVP=1:5)	1.500	10.035	0.300	
	B1 (YAG:5%Eu^{3+}/PVP=1:1)	0.300	2.200		0.300
S_{a4}	A1 ($CoFe_2O_4$/PVP=1:1)	0.300	2.007	0.300	
	B2(YAG:5%Eu^{3+}/PVP=1:2)	0.600	4.400		0.300
S_{a5}	A1 ($CoFe_2O_4$/PVP=1:1)	0.300	2.007	0.300	
	B3(YAG:5%Eu^{3+}/PVP=1:3)	0.900	6.600		0.300
S_{a6}	A1 ($CoFe_2O_4$/PVP=1:1)	0.300	2.007	0.300	

	B4 (YAG:5%Eu^{3+}/PVP=1:5)	1.500	11.000		0.300
S_{b1}	Mixing A1 and B1	0.600	4.207	0.300	0.300

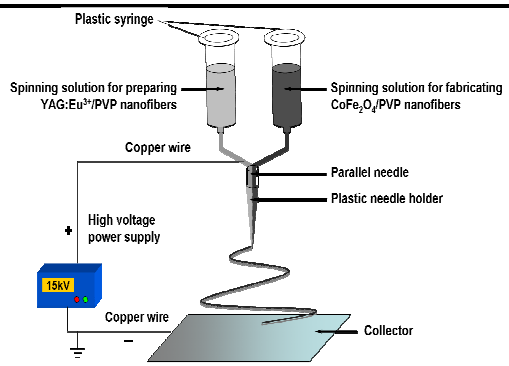

Fig. 1 Schematic diagram of the homemade parallel spinneret and the electrospinning setup

3 Characterization

The samples were identified by an X-ray powder diffractometer (XRD, Bruker D8 FOCUS) with Cu Kα radiation, and the operation voltage and current were kept at 40 kV and 20 mA, respectively. The morphology and internal structure of samples were observed by a field emission scanning electron microscope (SEM, XL-30) and a transmission electron microscope (TEM, JEM-2010), respectively. The luminescent properties of samples were investigated by a Hitachi fluorescence spectrophotometer F-7000. The magnetic performance of samples was measured by a vibrating sample magnetometer (VSM, MPMS SQUID XL). The ultraviolet-visible diffuse reflectance spectrum of the sample was determined by a UV-1240 ultraviolet-visible spectrophotometer. All measurements were performed at room temperature.

4 Results and Discussion

4.1 Crystal structure

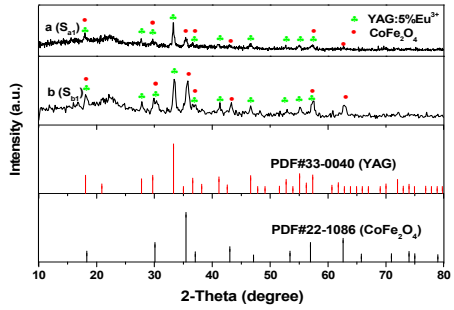

Fig. 2 XRD patterns of [$CoFe_2O_4$/PVP]//[YAG:5%Eu^{3+}/PVP] Janus nanofibers (S_{a1}) (a) and $CoFe_2O_4$/YAG:5%Eu^{3+}/PVP composite nanofibers (S_{b1}) (b) with PDF standard cards of YAG and $CoFe_2O_4$

The phase compositions of [$CoFe_2O_4$/PVP]//[YAG:5%Eu^{3+}/PVP] Janus nanofibers (S_{a1}) and $CoFe_2O_4$/YAG:5%Eu^{3+}/PVP composite nanofibers (S_{b1}) are characterized by means of XRD analysis, as shown in **Fig. 2**. It can be seen that XRD patterns of [$CoFe_2O_4$/PVP]//[YAG:5%Eu^{3+}/PVP] Janus nanofibers and $CoFe_2O_4$/YAG:5%Eu^{3+}/PVP composite nanofibers are conformed to the cubic phase with primitive structure of YAG (PDF#33-0040) and the cubic spinel structure of $CoFe_2O_4$ (PDF#22-1086), and the diffraction peak of the amorphous PVP (2θ=22.2°) also can be observed, indicating that [$CoFe_2O_4$/PVP]//[YAG:5%Eu^{3+}/PVP] Janus nanofibers and $CoFe_2O_4$/YAG:5%Eu^{3+}/PVP composite nanofibers contain crystalline YAG:7%Tb^{3+}, $CoFe_2O_4$ and amorphous PVP.

4.2 Morphology

The morphologies of the as-prepared $CoFe_2O_4$ nanofibers (S_1) and YAG:5%Eu^{3+} nanofibers (S_2) are observed by means of SEM, as presented in **Fig. 3a** and **Fig. 3b**. $CoFe_2O_4$ nanofibers and YAG:5%Eu^{3+} nanofibers have coarse surface, and the size distribution of the as-prepared nanofibers are almost uniform, and the diameters of the $CoFe_2O_4$ nanofibers and YAG:5%Eu^{3+} nanofibers are 81.43±9.2 nm and 126.84±16.9 nm under the confidence level of 95%, respectively, as demonstrated in **Fig. 4a** and **Fig. 4b**. The morphologies and structures of [$CoFe_2O_4$/PVP]//[YAG:5%Eu^{3+}/PVP] Janus nanofibers (S_{a1}) and $CoFe_2O_4$/YAG:5%Eu^{3+}/PVP composite nanofibers (S_{b1}) are characterized by the combination of SEM and TEM analyses. As seen from **Fig. 3c**, **Fig. 3d** and **Fig. 3e**, the surface of the Janus nanofibers and composite nanofibers is smooth, and each [$CoFe_2O_4$/PVP]//[YAG:5%Eu^{3+}/PVP] Janus nanofiber consists of two nanofibers assembled side-by-side. The TEM image of [$CoFe_2O_4$/PVP]//[YAG:5%Eu^{3+}/PVP] Janus nanofibers is presented in **Fig. 3f**. One strand nanofiber of the Janus nanofiber is composed of $CoFe_2O_4$ magnetic nanofibers and PVP, and the other one consists of YAG:5%Eu^{3+} luminescent nanofibers and PVP. The mean diameter for individual nanofiber of the Janus nanofibers (Sa_1) is ca. 283.06±36.7 nm under the confidence level of 95%, as revealed in **Fig. 4c**. It can be observed from **Fig. 3g** that $CoFe_2O_4$ magnetic nanofibers and YAG:5%Eu^{3+} luminescent nanofibers are dispersed in the $CoFe_2O_4$/YAG:5%Eu^{3+}/PVP composite nanofibers. The diameter of the $CoFe_2O_4$/YAG:5%Eu^{3+}/PVP composite nanofibers (Sb_1) is 632.98±33.6 nm under the confidence level of 95%, as revealed in **Fig. 4d**. From the above SEM and TEM analyses, we can confirm that the [$CoFe_2O_4$/PVP]//[YAG:5%Eu^{3+}/PVP] Janus nanofibers have been successfully fabricated. As seen from **Fig. 3h**, one can see that the Janus nanofibers are flexible nanofibers.

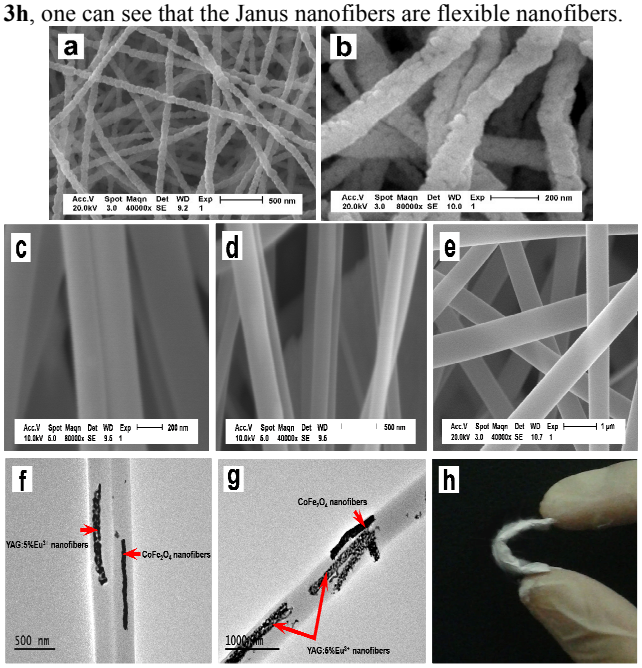

Fig. 3 SEM images of $CoFe_2O_4$ nanofibers (S_1) (a), YAG:5%Eu^{3+} nanofibers (S_2) (b), and SEM images and TEM images of [$CoFe_2O_4$/PVP]//[YAG:5%Eu^{3+}/PVP] Janus nanofibers (S_{a1}) (c, d, e), $CoFe_2O_4$/YAG:5%Eu^{3+}/PVP composite nanofibers (S_{b1}) (f, g) and photograph of [$CoFe_2O_4$/PVP]//[YAG:5%Eu^{3+}/PVP] flexible Janus nanofibers (h)

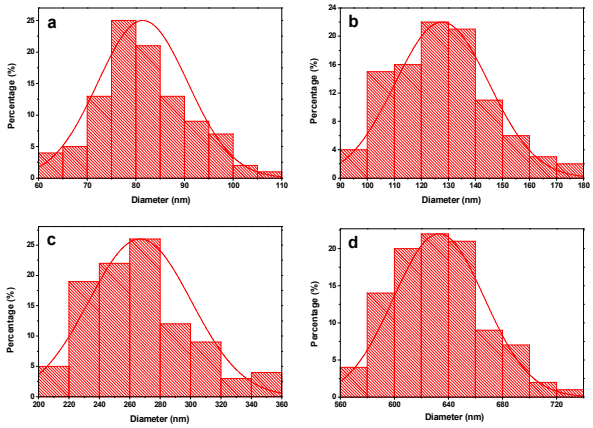

Fig. 4 Histograms of diameters distribution of $CoFe_2O_4$ nanofibers (S_1) (a), YAG:5%Eu^{3+} nanofibers (S_2) (b), [$CoFe_2O_4$/PVP]//[YAG:5%Eu^{3+}/PVP] Janus nanofibers (S_{a1}) (c) and $CoFe_2O_4$/YAG:5%Eu^{3+}/PVP composite nanofibers (S_{b1}) (d)

4.3 Luminescent properties of [$CoFe_2O_4$/PVP]//[YAG:5%Eu^{3+}/PVP] Janus nanofibers

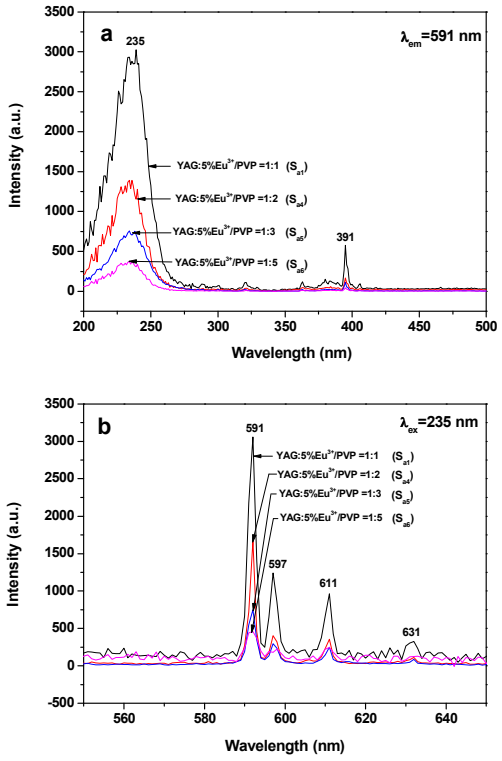

Fig. 5 Excitation spectra (a) and emission spectra (b) of [$CoFe_2O_4$/PVP]//[YAG:5%Eu^{3+}/PVP] Janus nanofibers (S_{a1}, S_{a4}, S_{a5} and S_{a6}) containing different mass ratios of YAG:5%Eu^{3+} nanofibers to PVP when the mass ratio of $CoFe_2O_4$ nanofibers to PVP is fixed at 1:1

In order to investigate the impact of the mass ratio of YAG:5%Eu^{3+} luminescent nanofibers to PVP on the luminescent performance, a series of [$CoFe_2O_4$/PVP]//[YAG:5%Eu^{3+}/PVP] Janus nanofibers (S_{a1}, S_{a4}, S_{a5} and S_{a6}) were fabricated. In order to perform this study, the mass ratio of $CoFe_2O_4$ nanofibers to PVP is fixed as 1:1 and the mass ratios of YAG:5%Eu^{3+} nanofibers to PVP are varied from 1:1 to 1:5. It can be observed from **Fig. 5a** that the excitation spectra (monitored by 591 nm) of the samples show the predominant excitation band (200-300 nm) centering at 235 nm is assigned to the charge transfer from the 2p orbital of O^{2-} ions to the 4f orbital of Eu^{3+} ions, while the sharp excitation peak at 391 nm is due to the $^7F_0 \rightarrow {}^5L_6$ transition of Eu^{3+} ions. As shown in **Fig. 5b**, characteristic emission peaks of Eu^{3+} are observed under the excitation of 235-nm ultraviolet light and ascribed to the energy levels transitions of $^5D_0 \rightarrow {}^7F_1$ (591 nm), $^5D_0 \rightarrow {}^7F_1$ (597 nm), $^5D_0 \rightarrow {}^7F_2$ (611 nm) and $^5D_0 \rightarrow {}^7F_2$ (631 nm) of Eu^{3+} ions, and the $^5D_0 \rightarrow {}^7F_1$ energy levels transition at 591 nm is the predominant emission peak. It is found from **Fig. 5** that the peaks have the same spectral shape with the increase of amount of luminescent substance, whereas the intensities of excitation and emission peaks are strengthened, indicating that the luminescent intensity of the Janus nanofibers can be tuned by adjusting the amount of luminescent material.

The excitation spectra (monitored at 591 nm) and emission spectra (excited by 235 nm) of [$CoFe_2O_4$/PVP]//[YAG:5%Eu^{3+}/PVP] Janus nanofibers (S_{a1}, S_{a2} and S_{a3}) containing different amounts of $CoFe_2O_4$ magnetic nanofibers are indicated in **Fig. 6**. In order to perform this investigation, the mass ratio of YAG:5%Eu^{3+} nanofibers to PVP is fixed as 1:1 and the mass ratios of $CoFe_2O_4$ nanofibers to PVP are varied from 1:1 to 1:5. As seen from **Fig. 6**, the excitation and emission intensity of [$CoFe_2O_4$/PVP]//[YAG:5%Eu^{3+}/PVP] Janus nanofibers are decreased with the increase of the amount of $CoFe_2O_4$ nanofibers introduced into the Janus nanofibers. This phenomenon may result from the light absorbance of the dark-colored $CoFe_2O_4$ nanofibers. From the ultraviolet-visible diffuse reflectance spectrum of $CoFe_2O_4$ nanofibers (S_1) illustrated in **Fig. 7**, it is observed that $CoFe_2O_4$ nanofibers can absorb light at ultraviolet wavelengths (<400 nm) much more strongly than visible range (400-700 nm). Both the exciting light (235 nm) and emitting light (591-631 nm) can be absorbed by dark-colored $CoFe_2O_4$. Thus, the exciting light and emitting light are absorbed by the $CoFe_2O_4$ nanofibers, resulting in the decrease in the intensity of excitation and emission peaks. Furthermore, the more $CoFe_2O_4$ nanofibers introduced into the Janus nanofibers, the more decrease in the intensity of excitation and emission peaks.

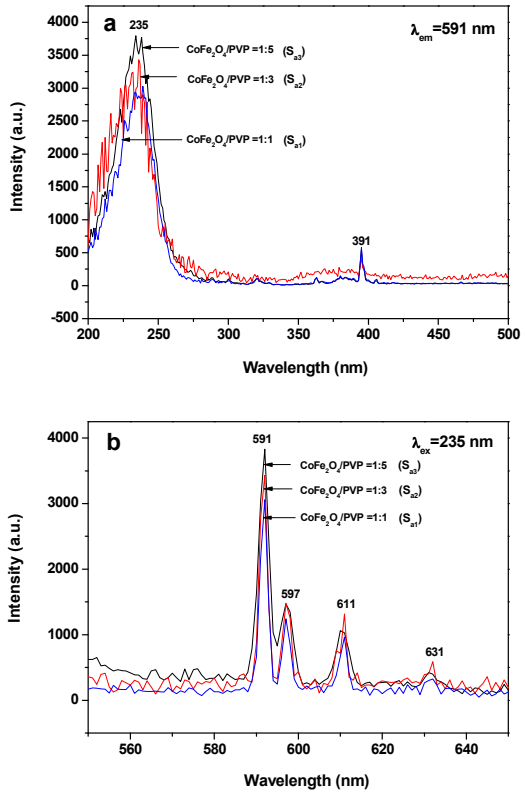

Fig. 6 Excitation spectra (a) and emission spectra (b) of [$CoFe_2O_4$/PVP]//[YAG:5%Eu^{3+}/PVP] Janus nanofibers (S_{a1}, S_{a2} and S_{a3}) containing different mass ratios of $CoFe_2O_4$ nanofibers to PVP when the mass ratio of YAG:5%Eu^{3+} to PVP is fixed at 1:1

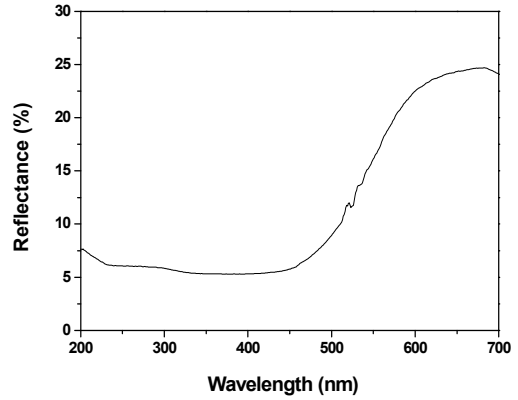

Fig. 7 UV-vis diffuse reflectance spectrum of $CoFe_2O_4$ nanofibers (S_1)

To illustrate the advantages of the nanostructure of the magnetic-luminescent bifunctional Janus nanofibers, the $CoFe_2O_4$/YAG:5%Eu^{3+}/PVP composite nanofibers (S_{b1}), as a contrast sample, were also fabricated by mixing the spinning solution A1 ($CoFe_2O_4$/PVP=1:1) and the spinning solution B1 (YAG:5%Eu^{3+}/PVP=1:1) together followed by electrospinning via the traditional single-spinneret electrospinning setup. From the contrast between the Janus nanofibers (S_{a1}) ($CoFe_2O_4$/PVP=1:1, YAG:5%Eu^{3+}/PVP=1:1) and $CoFe_2O_4$/YAG:5%Eu^{3+}/PVP composite nanofibers (S_{b1}) which have the same components, as shown in **Fig. 8**, one can see that emission intensity of the Janus nanofibers is much stronger than that of $CoFe_2O_4$/YAG:5%Eu^{3+}/PVP composite nanofibers. This result can be attributed to the isolation of YAG:5%Eu^{3+} from $CoFe_2O_4$. As illustrated in **Fig. 9**, YAG:5%Eu^{3+} nanofibers and $CoFe_2O_4$ nanofibers are promiscuously dispersed in the $CoFe_2O_4$/YAG:5%Eu^{3+}/PVP composite nanofiber. The exciting light in the composite nanofiber has to pass through $CoFe_2O_4$ nanofibers to reach and excite YAG:5%Eu^{3+} nanofibers. In this process, a large part of the exciting light has been absorbed by $CoFe_2O_4$ nanofibers, and thus the exciting light is much weakened before it reaches the YAG:5%Eu^{3+} nanofibers. Similarly, the emitting light emitted by YAG:5%Eu^{3+} nanofibers also has to pass through $CoFe_2O_4$ nanofibers and is absorbed by them. Consequently, both the exciting and emitting light are severely weakened. For the [$CoFe_2O_4$/PVP]//[YAG:5%Eu^{3+}/PVP] Janus nanofibers, YAG:5%Eu^{3+} nanofibers and $CoFe_2O_4$ nanofibers are separated in their own strand, so that the exciting light and emitting light in the YAG:5%Eu^{3+} nanofibers strand will be little affected by $CoFe_2O_4$ nanofibers. The overall effect is that the [$CoFe_2O_4$/PVP]//[YAG:5%Eu^{3+}/PVP] Janus nanofibers possess much higher luminescent performance than the $CoFe_2O_4$/YAG:5%Eu^{3+}/PVP composite nanofibers.

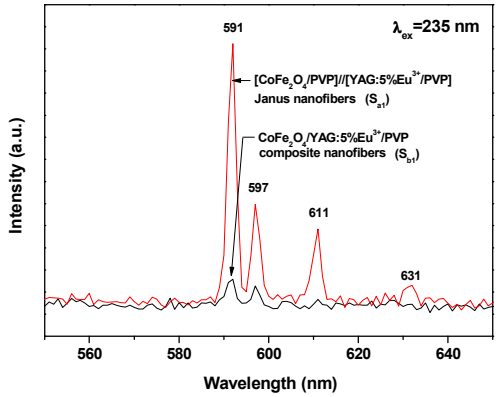

Fig. 8 Emission spectra of [$CoFe_2O_4$/PVP]//[YAG:5%Eu^{3+}/PVP] Janus nanofibers (S_{a1}) and $CoFe_2O_4$/YAG:5%Eu^{3+}/PVP composite nanofibers (S_{b1})

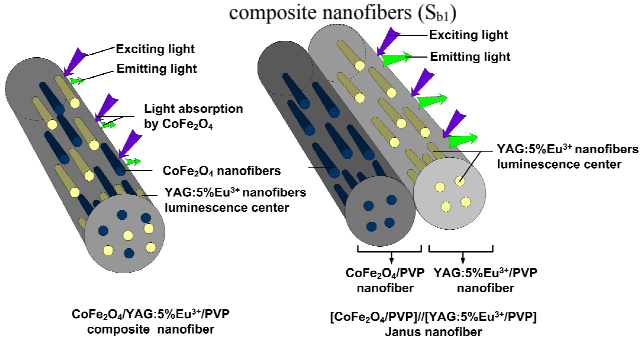

Fig. 9 Schematic diagram of the situation of the exciting light and emitting light in $CoFe_2O_4$/YAG:5%Eu^{3+}/PVP composite nanofiber and [$CoFe_2O_4$/PVP]//[YAG:5%Eu^{3+}/PVP] Janus nanofiber

4.4 Magnetic properties of [$CoFe_2O_4$/PVP]//[YAG:5%Eu^{3+}/PVP] Janus nanofibers

The typical hysteresis loops for $CoFe_2O_4$ nanofibers (S_1), [$CoFe_2O_4$/PVP]//[YAG:5%Eu^{3+}/PVP] Janus nanofibers (S_{a1}, S_{a2} and S_{a3}) containing different mass ratios of $CoFe_2O_4$ nanofibers

to PVP and $CoFe_2O_4$/YAG:5%Eu^{3+}/PVP composite nanofibers (S_{b1}) are shown in **Fig. 10**, and the saturation magnetizations of the samples are summarized in **Table 2**. As seen from **Fig. 10**, the saturation magnetization of the $CoFe_2O_4$ nanofibers is 41.34 emu·g^{-1}, which is similar to the data reported by previous literatures [14-16]. The saturation magnetization of [$CoFe_2O_4$/PVP]//[YAG:5%Eu^{3+}/PVP] Janus nanofibers containing different mass ratios of $CoFe_2O_4$ nanofibers to PVP are 20.32 emu·g^{-1}, 6.73 emu·g^{-1} and 3.12 emu·g^{-1}, respectively, as revealed in **Fig. 10** and **Table 2**. It is known that the saturation magnetization of a magnetic composite material depends on the mass percentage of the magnetic substance in the magnetic composite material [21-23]. It is found that the saturation magnetization of the [$CoFe_2O_4$/PVP]//[YAG:5%Eu^{3+}/PVP] Janus nanofibers is increased with the increase of the amount of $CoFe_2O_4$ magnetic nanofibers introduced into the $CoFe_2O_4$/PVP strand, implying that the magnetism of the Janus nanofibers can be tunable by adjusting the amount of $CoFe_2O_4$ magnetic nanofibers. The saturation magnetization of the $CoFe_2O_4$/YAG:5%Eu^{3+}/PVP composite nanofibers is 20.53 emu·g^{-1}, which is close to that of the Janus nanofibers marked c (20.32 emu·g^{-1}) in **Fig. 10**. Combined luminescence with magnetism analysis, it is found that when the Janus nanofibers have the close magnetic property to the $CoFe_2O_4$/YAG:5%Eu^{3+}/PVP composite nanofibers, the luminescent intensity of the Janus nanofibers is much higher than that of the composite nanofibers, demonstrating that the novel Janus nanofibers have better magnetic-luminescent performance than the composite nanofibers.

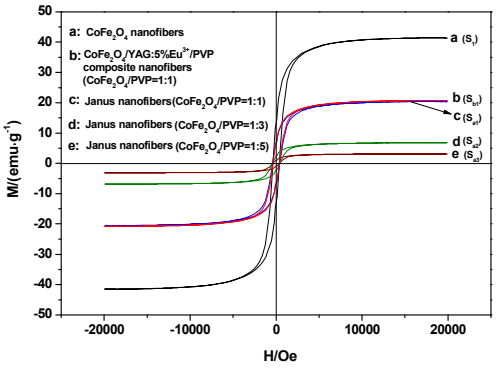

Fig. 10 Hysteresis loops of $CoFe_2O_4$ nanofibers (S_1) (a), $CoFe_2O_4$/YAG:5%Eu^{3+}/PVP composite nanofibers (S_{b1}) (b) and [$CoFe_2O_4$/PVP]//[YAG:5%Eu^{3+}/PVP] Janus nanofibers (S_{a1}, S_{a2} and S_{a3}) containing different mass ratios of $CoFe_2O_4$ nanofibers to PVP (c, d, e)

Table 2 Saturation magnetization of samples

Samples	Saturation magnetization (Ms)/(emu·g^{-1})
$CoFe_2O_4$ nanofibers (S_1)	41.34
$CoFe_2O_4$/YAG:5%Eu^{3+}/PVP composite nanofibers (S_{b1}) ($CoFe_2O_4$/PVP=1:1)	20.53
[$CoFe_2O_4$/PVP]//[YAG:5%Eu^{3+}/PVP] Janus nanofibers (S_{a1}) ($CoFe_2O_4$/PVP=1:1)	20.32
[$CoFe_2O_4$/PVP]//[YAG:5%Eu^{3+}/PVP] Janus nanofibers (S_{a2}) ($CoFe_2O_4$/PVP=1:3)	6.73
[$CoFe_2O_4$/PVP]//[YAG:5%Eu^{3+}/PVP] Janus nanofibers (S_{a3}) ($CoFe_2O_4$/PVP=1:5)	3.12

5 Conclusions

In summary, magnetic-luminescent bifunctional [$CoFe_2O_4$/PVP]//[YAG:5%Eu^{3+}/PVP] Janus nanofibers have been successfully synthesized by electrospinning technology using a homemade parallel spinneret. One strand nanofiber of the Janus nanofiber is composed of $CoFe_2O_4$ magnetic nanofibers and PVP, and the other one consists of YAG:5%Eu^{3+} luminescent nanofibers and PVP. The average diameter of each strand of the Janus nanofiber is ca. 283.06±36.7 nm. It is very gratifying to see that the magnetic-luminescent bifunctional Janus nanofibers simultaneously possess excellent luminescent performance and magnetic properties. Furthermore, the luminescent intensity and magnetism of the Janus nanofibers can be tuned via adjusting the content of luminescent and magnetic compounds. Besides, the design conception and preparation method of the Janus nanofibers are of universal significance to fabricate other one-dimensional multifunctional nanostructures. The new high-performance [$CoFe_2O_4$/PVP]//[YAG:5%Eu^{3+}/PVP] magnetic-luminescent bifunctional Janus nanofibers have potential applications in the fields of medical diagnostics, drug target delivery, optical imaging, anti-counterfeiting technology and future nanomechanics.

Acknowledgments

This work was financially supported by the National Natural Science Foundation of China (NSFC 50972020, 51072026), Specialized Research Fund for the Doctoral Program of Higher Education (20102216110002, 20112216120003), the Science and Technology Development Planning Project of Jilin Province (Grant Nos. 20130101001JC, 20070402), the Science and Technology Research Project of the Education Department of Jilin Province during the eleventh five-year plan period(Under grant No. 2010JYT01), Key Research Project of Science and Technology of Ministry of Education of China (Grant No. 207026).

Notes and references

Key Laboratory of Applied Chemistry and Nanotechnology at Universities of Jilin Province, Changchun University of Science and Technology, Changchun 130022. Fax: 86 0431 85383815; Tel: 86 0431 85582574; E-mail: dongxiangting888@163.com

1. W. Wang, Z. Y. Li, X. R. Xu, B. Dong, H. N. Zhang, Z. J. Wang, C. Wang, R. H. Baughman and S. L. Fang, *Small,* 2011, **7**, 597.
2. W. Wang, M. Zou, K. Z. Chen, *Chem. Commun.*, 2010, **46**, 5100.
3. J. Feng, S. Y. Song, R. P. Deng, W. Q. Fan, H. J. Zhang, *Langmuir*, 2010, **26**, 3596.
4. H. Y. Chen, D. C. Colvin, B. Qi, T. Moore, J. He, O. T. Mefford, F. Alexis, J. C. Gore and J. N. Anker, *J. Mater. Chem.*, 2012, **22**, 12802.
5. P. Lu, J. L. Zhang, Y. L. Liu, D. H. Sun, G. X. Liu, G. Y. Hong and J. Z. Ni, *Talanta*, 2010, **83**, 450.
6. H. G. Wang, L. Sun, Y. P. Li, X. L. Fei, M. D. Sun, C. Q. Zhang, Y. X. Li and Q. B. Yang, *Langmuir*, 2011, **27**, 11609.
7. P. Sun, H. Y. Zhang, C. Liu, J. Fang, M. Wang, J. Chen, J. P. Zhang,

C. B. Mao and S. K. Xu, Langmuir, 2010, **26**, 1278.
8. F. Grasset, F. Dorson, Y. Molard, S. Cordier, V. Demange, C. Perrin, V. Marchi-Artzner and H. Haneda, *Chem. Commun.*, 2008, **39**, 4729.
9. L. N. Chen, J. Wang, W. T. Li and H. Y. Han, *Chem. Commun.*, 2012, **48**, 4971.
10. X. M. Li, X. Xing, W. J. Yang, W. L. Li and L. F. Kong, *Semiconductor Optoelectronics*, 2010, **31**, 71.
11. R. Lopez, E. A. Aguilar and J. Zarate-Medina, *J. Eur. Ceram. Soc.*, 2010, **30**, 73.
12. P. F. S. Pereira, M. G. Matos, L. R. Ávila, E. C. O. Nassor, A. Cestari, K. J. Ciuffi, P. S. Calefi and E. J. Nassar, *J. Lumin*., 2010,**130**, 488.
13. H. K. Yang and J. H. Jeong, *J. Phys. Chem. C*, 2010, **114**, 226.
14. J. C. Fu, J. L. Zhang, Y. Peng, J. G. Zhao, G. G. Tan, N. J. Mellors, E. Q. Xie and W .H. Han, *Nanoscale*, 2012, **4**, 3932.
15. C. Fernandes, C. Pereira, M. P. F. García, A. M. Pereira, A. Guedes, R. F. Pacheco, A. Ibarra, M. R. Ibarra, J. P. Araújo and C. Freire, *J. Mater. Chem. C*, 2014, **2**, 5818.
16. Q. Cao, Z. W. Liu and R. C. Che, *New J. Chem.*, 2014, **38**, 3193.
17. H. Wang, Y. Li, L. Sun, Y. Li, W. Wang, S. Wang, S. Xu and Q. Yang, J. *Colloid Interface Sci.,* 2010, **350**, 396.
18. Z. Y. Hou, C. X. Li, P. G. Ma, G. G. Li, Z. Y. Cheng, C. Peng, D. M. Yang, P. P. Yang and J. Lin, *Adv. Funct. Mater.*, 2011, **21**, 2356.
19. J. B. Mu, C. L. Shao, Z. C. Guo, Z. Y. Zhang, M. Y. Zhang, P. Zhang, B. Chen and Y. C. Liu, *Appl. Mater. Interfaces*, 2011, **3**, 590.
20. J. Song, M. L. Chen, M. B. Olesen, C. X. Wang, R. Havelund, Q. Li, E. Q. Xie, R. Yang, P. Bøggild, C. Wang, F. Besenbacher and M. D. Dong, *Nanoscale*, 2011, **3**, 4966.
21. N. Lv, Q. L. Ma, X. T. Dong, J. X. Wang, W. S. Yu and G. X. Liu, *Chem. Eng. J.*, 2014, **243**, 500.
22. S. L. Chen, H. Q. Hou, F. Harnisch, S. A. Patil, A. A, *Energy Environ. Sci.*, 2011, **4**, 1417.
23. N. Lv, Q. L. Ma, X. T. Dong, J. X. Wang, W. S. Yu and G. X. Liu, *ChemPlusChem*, 2014, **79**, 690.
24. Q. L. Ma, W. S. Yu, X. T. Dong, J. X. Wang and G. X. Liu, *Nanoscale*, 2014, **6**, 2945.
25. Q. L. Ma, J. X. Wang, X. T. Dong, W. S. Yu and G. X. Liu, *ChemPlusChem*, 2014, **79**, 290.
26. X. Xi, J. X. Wang, X. T. Dong, Q. L. Ma, W. S. Yu and G. X. Liu, *Chem. Eng. J.*, 2014, **254**, 259.
27. T. Nisisako, T. Torii, T. Takahashi and Y. Takizawa, *Adv. Mater.* 2006, **18**, 1152.
28. H. R. Kyung, C. M. David and L. Joerg, *Nat. Mater.*, 2005, **4**, 759.
29. S. Isaac, Y. Xin, J. C. Emily, M. M. Nicholas, T. M. Gerald, K. Olga and C. B. Anna, *ACS Nano.*, 2013, **7**, 1224.